Journal of Building Technology, 2026, Volume 8, Issue 2
DOI: 10.32629/jbt.v8i2.5619
ISSN Online: 2717-5103
ISSN Print: 2705-1390

Analysis of an RC beam-column joint by the finite element method to define an efficient reinforcement

Jorge Luis Medina Torrez, Álvaro Moscoso Wayar*

Private University of Bolivia
*Corresponding Author:
Email address: alvaromoscoso@upb.edu

Abstract: The beam-column joint is a critical region on the reinforced concrete (RC) frame structural system due the critical tasks that it accomplishes and load conditions to which it is subjected. Its reduced geometry and the material's bond interaction of which the beam-column joint is compounded results in a non-linear behavior that is influenced by several variables. In this study, the mechanical behavior of the beam-column joint in Serviceability Limit State (ELS) is analyzed by means of a numerical model of finite elements. A comparison between the results obtained and those reported by other authors (experimental and numerical) is presented in order to validate the numerical model developed. The results showed that crack propagation due the negative bending moment on the beam significantly decreases the stiffness and introduces an increase of stresses on the joint. An open stirrups configuration in the upper half of the depth of the beam is proposed in order to control crack propagation.

Key words: beam column-joint; finite element; cracking; numerical analysis; reinforced concrete

1 Introduction

Beam-column joints (BCJ) are regions that exhibit a geometric discontinuity [1,2] where abrupt changes in stresses and in the transmission of various forces from the elements adjacent to the node occur [1]. Due to their critical role, particularly under cyclic lateral loads and monotonic gravitational loads, they are one of the main focuses of research in the study of reinforced concrete structures [3,4].

Although codes, such as ACI-352, provide recommendations for the design of beam-column joints, the specialized literature highlights that the load-bearing capacity and mechanical performance depend on more variables than those considered by the aforementioned code. At the same time, specialized studies reveal a lack of attention to the reinforcement of these joints in construction practice, leading to failures that can result in structural collapse [5,6].

This reality has prompted research into BCJs through experimental studies and numerical analyses that allow for a more precise understanding of stress distribution and deformations, as well as a more accurate replication of the complex behavior of these structural elements. One of the most suitable numerical methods for this type of analysis is the finite element method [7].

Park & Paulay [8] list the requirements they consider necessary for the satisfactory performance of reinforced concrete BCJs: (a) The joint must perform under service loads equal to that of the adjacent members, (b) the joint must

Copyright © 2026 by author(s) and Frontier Scientific Research Publishing Inc.
This work is licensed under the Creative Commons Attribution International License (CC BY 4.0).
http://creativecommons.org/licenses/by/4.0/

have a strength corresponding to the most adverse load combinations that the members it connects can withstand, (c) the strength of the joint must not limit the strength of the structure, and its behavior must not prevent the adjacent members from reaching their load-bearing capacity, (d) the design must allow for ease of construction and easy access for concrete placement. Haach [3] and Alva [4] identify the most important variables affecting the performance of the BCJ, which are listed below: (a) the degree of confinement of the connection, (b) the reinforcement arrangement, (c) the axial load on the column and its magnitude, (d) the concrete strength, (e) the geometric properties of the joint, and (f) the anchorage of the beams' longitudinal reinforcement.

With the aim of classifying beam-column connections, Roeser [9] tested eight external BCJs and seven internal BCJs, all with the same external dimensions but with different amounts of reinforcement, as shown in Figure. 1. He was then able to identify more and less ductile connections based on an evaluation of the load-strain curve for each connection. Among the tested configurations, those classified as RK2 and RK3 exhibited better performance. The reinforcement configurations of these two models were used by Lamas [10] to demonstrate the improvement in the mechanical performance of the connection that certain reinforcement configurations provide compared to the BCJ without additional reinforcement.

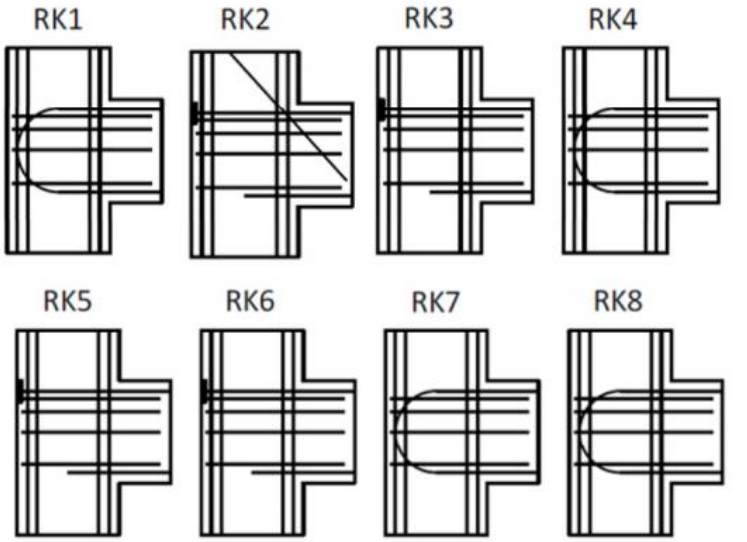


Figure 1. BCJ models from Roeser's experiments

Alva [4] and Ortiz [11], among other authors, point out that the mechanical deterioration of the BCJ is linked to various phenomena occurring at the joint, including those related to the development of cracks at different loading stages, such as cracking during service, which is addressed by ACI 352, but whose requirements are limited only to those specified in ACI 318 for cracking and deflection in service for portal frame members [12], or the appearance of diagonal cracks in the joint core during advanced loading stages. Considering these cracking phenomena in BCJ models allows for an evaluation of their influence on structural response and the proposal of reinforcement configurations.

The state of the art regarding the analysis of BCJ behavior indicates that further studies are needed to gain a detailed understanding of the effect of additional reinforcement and thus optimize its placement and reinforcement configuration so that these configurations can be more efficient and easier to construct [13].

This research presents a study focused on the analysis of an external BCJ under ELS using finite elements, proposing several configurations that help define an efficient reinforcement scheme under ELS. The numerical BCJ model developed in this work was calculated and processed using a code written in Python by the author. To validate the numerical model, the results obtained were compared with experimental and numerical tests. A comparative analysis is presented between

the results obtained here and those reported by Roeser [9] in his experimental tests, as well as a second comparison with the numerical results of Lamas [10], who also compared his results with those of Roeser [9].

2 Considerations on beam-column joints

The ACI-352 standard defines the BCJ as the portion of the column located within the height of the highest beam reaching the joint and classifies these joints according to their location and, consequently, their degree of confinement in the braced system: External and Internal. In turn, the standard provides a sub-classification based on the loads: (a) Type 1: frame members designed to meet the strength requirements of ACI 318-02 (without significant inelastic deformations) and (b) Type 2: frame members designed to maintain their strength under alternating deformations in the inelastic range. For the verification of either of the two types of BCJs mentioned, the ACI-352 standard proposes considering a ultimate shear force (purely horizontal) obtained from the most unfavorable load combination.

Furthermore, for a Type 1 external BCJ, the code specifies the following minimum construction requirements to maintain the confinement of the BCJ: (a) Horizontal transverse reinforcement must be placed over the entire height of the connection. (b) At least two rows of transverse reinforcement must be placed between the bottom and top of the longitudinal reinforcement of the highest beam reaching the core. (c) The spacing of stirrups must not exceed 300 mm, and if the joint is part of a structural system that resists non-seismic horizontal loads, it must not exceed 150 mm.

The horizontal and vertical forces acting on the BCJ produce diagonal stress fields in the core, which are transmitted by the compression strut toward the columns [4]. This resistance mechanism forms the basis of the procedures proposed by ACI 352 [5,13]. The placement of stirrups in the joint allows horizontal forces in the BCJ to be transmitted to the columns; thanks to the confinement provided by the steel reinforcement, the compression strut works over its entire height [3]. Therefore, the absence of stirrups leads to the formation of cracks that extend along the length of the compression strut. When these cracks extend to the top of the joint, the compression strut loses its ability to distribute the internal compressive stresses, and the BCJ fails [11].

The mechanical deterioration of the BCJ under ELS causes cracks to form due to the negative bending moment acting on the beam adjacent to the node; these cracks originate in the tension zone of this member near the BCJ. If these cracks extend into the compression zone of the beam, the joint suffers a significant reduction in flexural stiffness, which leads to a significant increase in displacements since the stress transfer between the concrete and the steel has been altered [3], Figure 2.

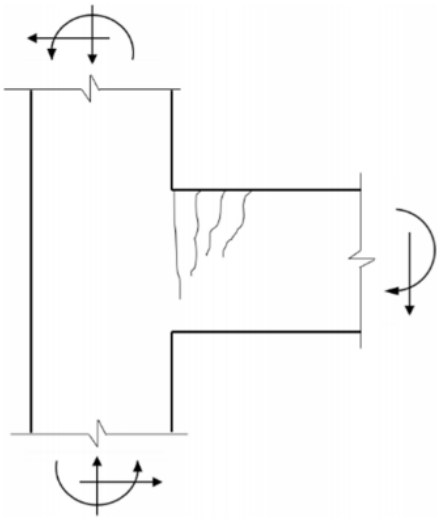


Figure 2. Cracking caused by the negative bending moment

3 Constitutive models and simplifications

The typical behavior of a concrete structural member can be described in three phases: (1) Linear elastic phase with uncracked concrete (Phase I), (2) Phase of initial cracking in the concrete (Phase II), and finally, (3) Material plasticization and failure phase (Phase III) [14,15].

In order to represent these three phases using the finite element method, the constitutive models for both concrete and steel must take the following into account: (a) Concrete under compression: Failure criterion, plasticization criterion, and hardening rule [16] (b) Concrete under tension: Loss of stiffness upon cracking, and the maximum stress criterion at which the concrete's stiffness changes [15]. This criterion corresponds to the phenomenon of "tension stiffening," which occurs when the steel resisting tensile stresses in a cracked region still transmits a portion of the stress to the surrounding concrete due to the bond between the materials, causing the concrete to bear tensile stresses [17]. (c) Steel: behaves as a perfectly elastic material.

The proposed numerical model focuses on Phases I and II of the behavior of a reinforced concrete member; therefore, material plasticization has not been considered, and only one criterion is taken into account, cracking for concrete under tension, with the aim of approximating the loss of stiffness experienced by the member as it transitions from Phase I to Phase II. The inclusion of this criterion requires that the analysis be performed in loading steps. All of the above considerations result in an approximation of the nonlinear behavior of reinforced concrete based on a simplified model, Figure 3.

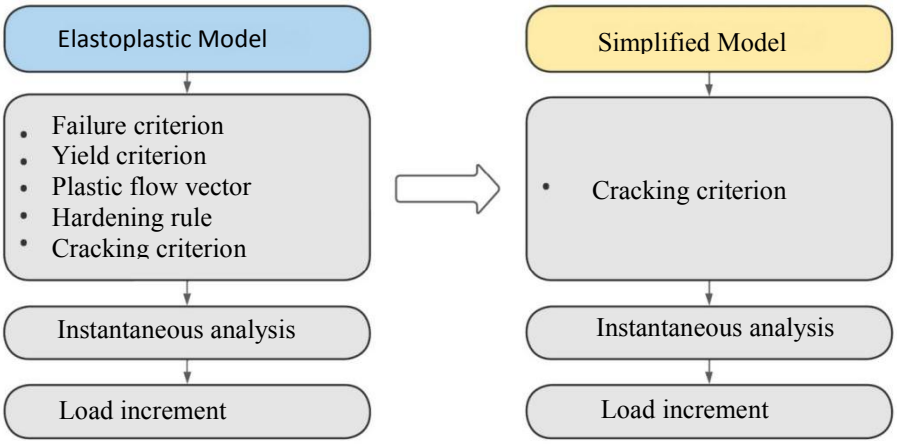


Figure 3. Simplification of the constitutive model for concrete

For the constitutive model of concrete under tension, a maximum stress criterion will be adopted, which will determine the limit of the material's elastic behavior and the loss of stiffness of the element. This limit will be evaluated based on principal stresses:

$$\sigma=\sigma_{1,2}=\frac{\sigma_x+\sigma_y}{2}\pm\sqrt{\left(\frac{\sigma_x-\sigma_y}{2}\right)^2+\tau_{xy}^2} \quad (1)$$

where σ1 is the maximum principal stress and σ_2 is the minimum. Thus, σ_1 will be the stress that determines whether or not an element has cracked.

4 Finite element model

To apply the finite element method, the problem has been considered in a plane stress state. In the initial loading stages, stresses and strains are linearly related via the constitutive matrix or the matrix of elastic constants D:

$$\{\sigma\}=[D]\{\varepsilon\} \quad (2)$$

The incorporation of the cracking criterion results in the modification of the stiffness matrices of the "cracked" elements during the loading steps as necessary according to the assumed cracking criterion. At each loading step, the system of equations generated by the system will take the form:

$$[K][u]=[f] \tag{3}$$

where [K] is the global stiffness matrix that is updated at each iteration; [u] are the displacements of the entire system at each step; and [f] are the external forces acting on the system.

The finite element used for concrete is a 4-node quadrilateral element, with 2 degrees of freedom per node, following the isoparametric formulation as shown in Figure 4 [18].

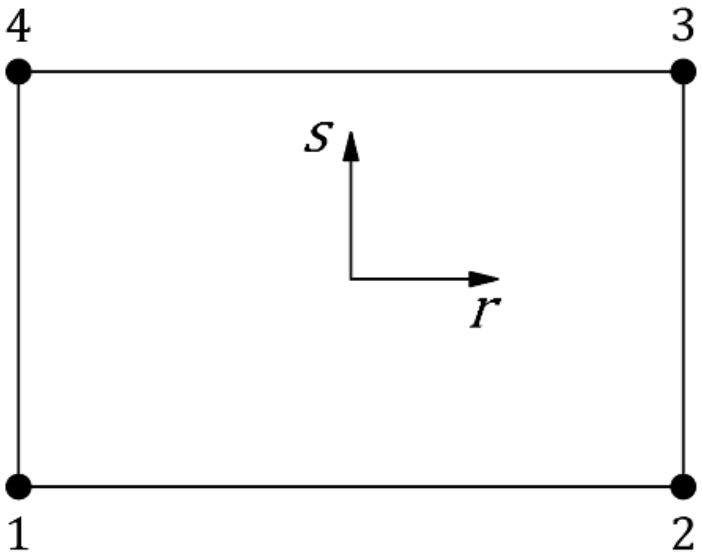


Figure 4. 4-node quadrilateral isoparametric element

The shape functions of the finite element are:

$$\begin{aligned} N_1(r,s) &= \tfrac{1}{4}(1-r)(1-s) \\ N_2(r,s) &= \tfrac{1}{4}(1+r)(1-s) \\ N_3(r,s) &= \tfrac{1}{4}(1+r)(1+s) \\ N_4(r,s) &= \tfrac{1}{4}(1-r)(1+s) \end{aligned} \tag{4}$$

To model the steel bars, a one-dimensional finite element with 2 nodes was used, with 2 degrees of freedom per node, which are associated with the following shape functions:

$$\begin{aligned} N_1(x) &= 1-x/L \\ N_2(x) &= x/L \end{aligned} \tag{5}$$

The computational data processing is described in Figure 5. Figure 6 presents the flowchart corresponding to the numerical application of the proposed cracking criterion. To avoid numerical singularity of the global matrix during the process, the stiffness loss coefficients of each element were calibrated until convergence with the experimental results was achieved, using the "Penalty Method."

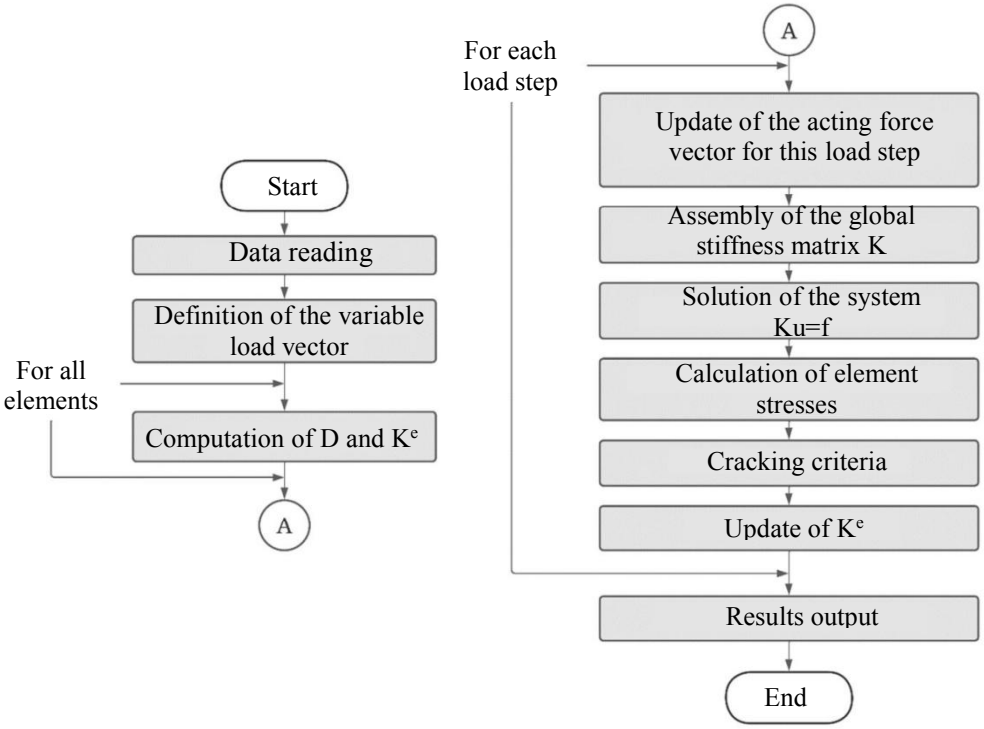


Figure 5. Main flowchart of the code

5 Strut-and-tie method

The strut-and-tie method is a procedure that allows for the design of structural concrete elements with geometric discontinuities [19]. This method involves idealizing a region D (discontinuity) of a structure by replacing it with a system consisting of isostatic articulated bars, which represent the behavior of that region. Due to their two-hinged nature, the bars are subjected solely to axial stress. The compressed bars are called tie rods and represent the concrete's compression zones. The tensioned bars are called struts and represent the tensile forces of the reinforcement [2].

For the study of reinforcement based on strut-and-tie models, two models derived from the simplification of Kassem's strut-and-tie model [13] have been used solely to propose reinforcement based on the resistance mechanisms of the joint. The first model considers the contribution of stirrups in the concrete core for resist horizontal shear, while the second considers the contribution that vertical bars located at the center of the joint could make to resist vertical shear, Figure 7.

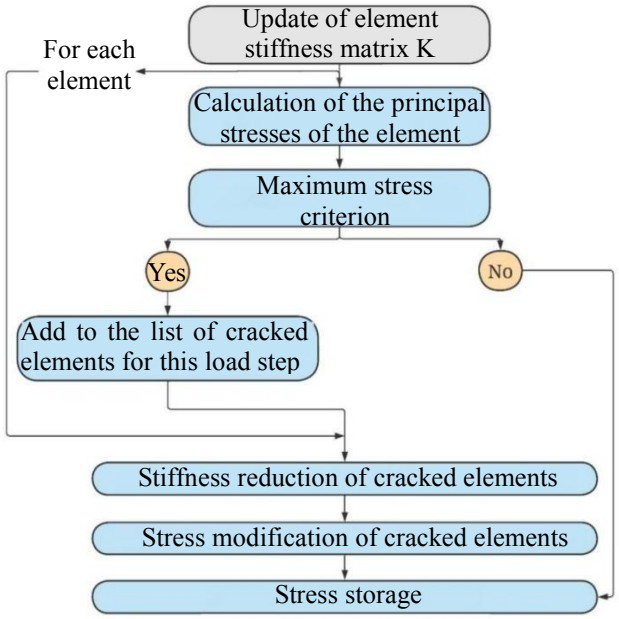


Figure 6. Application of cracking criteria in tensioned concrete

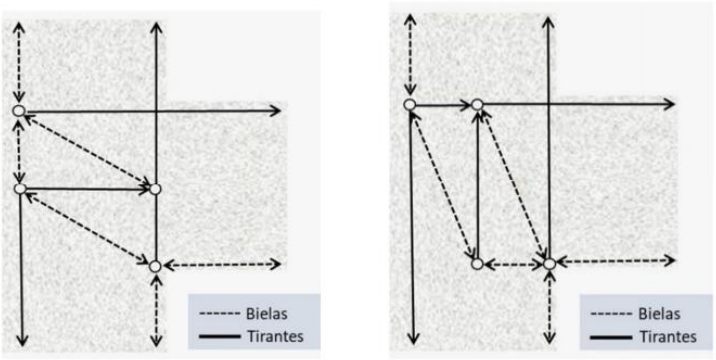


Figure 7. Model of a load-bearing truss with a horizontal strut in the core (left). Model of a load-bearing truss with a vertical strut in the core (right)

6 Validation and analysis performed

To validate the results, the BCJ models reported by Roeser [9] and Lamas [10] were reproduced. In all models, the assumed boundary conditions are: constraints on the "x" and "y" displacements at the bottom of the column and on the "x" displacement at the top of the column; a point load G at the top of the column; and a point load P at the end of the BCJ, as shown in Figure 8. The "load-displacement" analysis will be controlled from a node at the end of the beam, precisely where the monotonically varying load P is applied. These loads represent the conditions of an external BCJ subjected to predominantly gravitational loads, and whose behavior is limited to the service combination 1.0L + 1.0D for the specific case of this study.

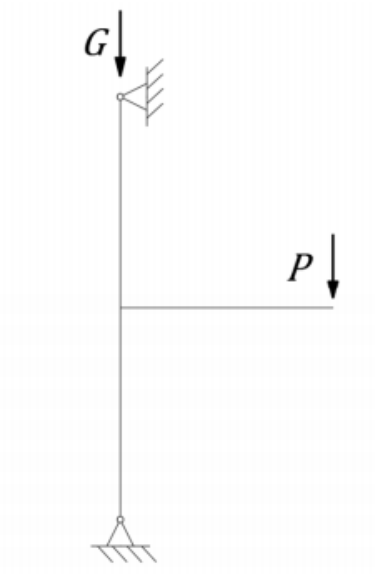


Figure 8. Boundary conditions and load system

Figure 9 and Table 1 present the characteristics of the BCJ RK2 model reported by Roeser. This model features a reinforcement configuration that meets the requirements of the code, plus additional reinforcement at the joint.

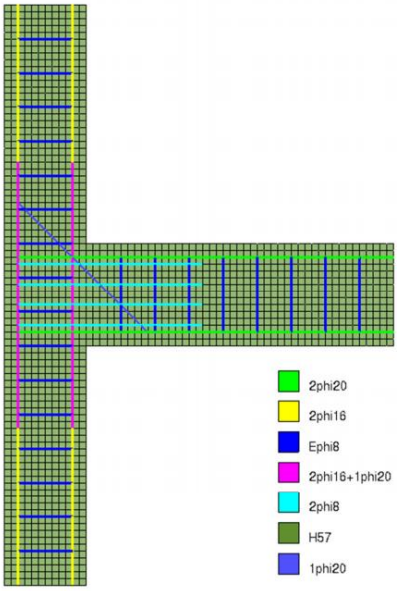


Figure 9. Finite element mesh of the RK2 model

Table 1. Material parameters (RK2 model)

Material	Compressive strength (MPa)	Tensile strength (MPa)	E (MPa)	Poisson's ratio
Concrete	57.4	5.3	324446	0.11
Steel	537 – 626	537 – 626	210000	0.3

Figure 10 and Table 2 present the characteristics of the BCJ models reported by Lamas [10] for BCJ. These are a variation of the RK2 model adapted to construction practices in our country.

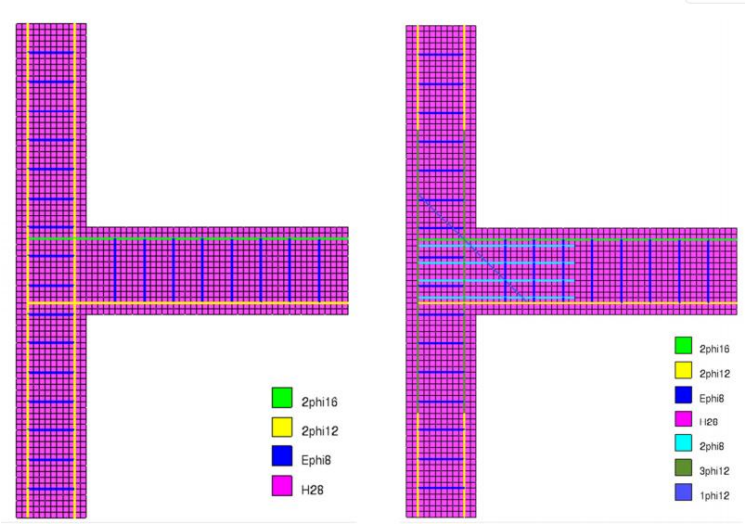


Figure 10. Finite element mesh of the SR model (left) and the CR model (right)

Table 2. Material parameters (SR and CR models)

Material	Compressive strength (MPa)	Tensile strength (MPa)	E (MPa)	Poisson's ratio
Concrete	28	3.7	24870	0.16
Steel	420	420	203000	0.3

After replicating the RK2 models by Roeser [9] and the SR and CR models by Lamas [10] for validation, additional models were developed based on the characteristics of the SR model plus additional reinforcement to evaluate its influence on the BCJ. To estimate the influence of closed stirrups at the joint, the specimens shown in Figure 11 were modeled and sorted according to their ratio (ρ_w, Eq. 6): 0.34% (SR), 0.5% (E1), 0.78% (E2).

$$\rho_w = A_{sw}/A_{cv} \tag{6}$$

where A_{cv} is the gross cross-sectional area of the beam and A_{sw} is the area of the stirrups at the joint.

The contribution of vertical bar reinforcement in the BCJ has been studied based on the analysis of the models shown in Figure 12 according to their amount of vertical reinforcement: 0.0% (SR), 0.47% (V1), 0.94% (V2), 1.41% (V3), with A_{cv} as the gross cross-sectional area of the column. These models are based on the conventional reinforcement configuration without additional steel reinforcement from the SR model.

Finally, six models with open stirrup configurations were developed to evaluate their influence on mechanical performance during service phases. In these models, the following variables are varied: (a) the number of stirrups and (b) their geometric arrangement. The first three models feature open steel stirrups placed symmetrically along the entire height of the beam. Figure 13 shows the models according to their steel content ρ_w as given by Equation 6, again with A_{cv} as the gross cross-sectional area of the beam and A_{sw} as the area of the open stirrups at the joint: 0.0% (SR), 0.38% (H1), 0.75% (H2), 1.13% (H3). Figure 14 shows the following three models with open stirrups placed only in the upper half of the beam's height, with ρ_w equal to: 0.0% (SR), 0.38% (H4), 0.75% (H5), 1.34% (H6).

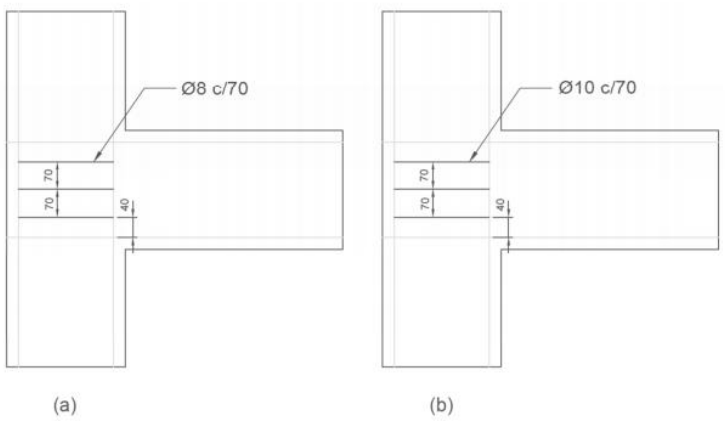


Figure 11. Specimens with closed stirrups: a) El, b) E2. (mm)

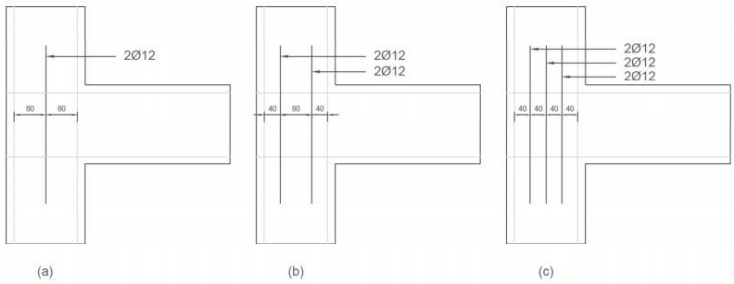


Figure 12. Specimens with vertical bars: a) Vl, b) V2, c) V3. (mm)

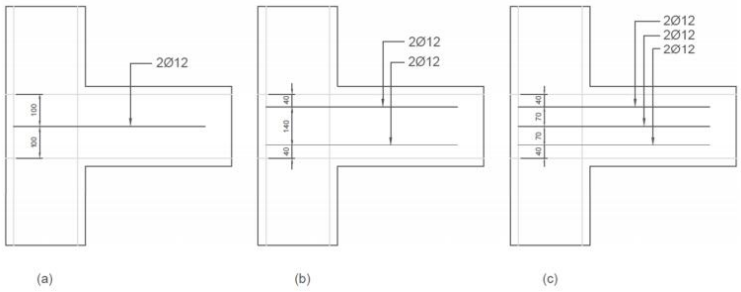


Figure 13. Specimens with open stirrups: a) H1, b) H2, c) H3. (mm)

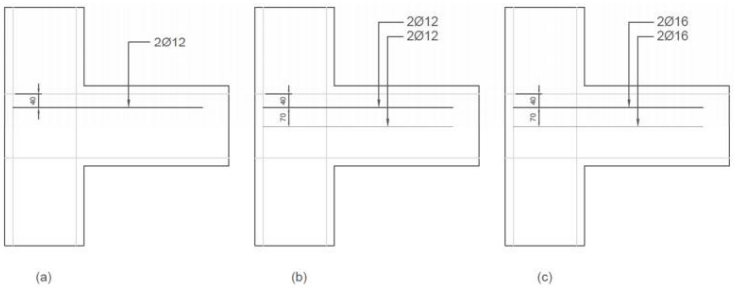


Figure 14. Specimens with open stirrups: a) H4, b) H5, c) H6. (mm)

7 Discussion of results

(a) Validation of the numerical model: Figure 15 shows a comparison of the load-displacement curves reported by Lamas [10] and Roeser [9] with the curve obtained by the numerical model developed in this study, "Medina RK2."

Convergence of results can be observed up to 50 kN, assuming a stiffness reduction coefficient of 1% in all cracked elements for each load step. This result meets the convergence expectations for phases I and II [15].

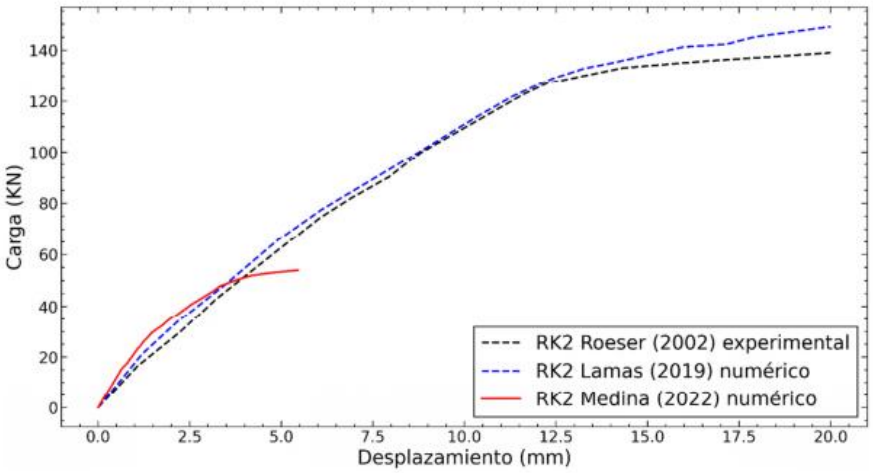


Figure 15. Load-displacement diagrams for the RK2 model

Figure 16 again shows a convergence between the "Medina SR" and "Medina CR" curves and the curves reported by Lamas [10] up to a load level of 36 kN; this is because plasticization effects become significant starting at that load stage.

(b) Study of the joint's behavior under the influence of different numbers of closed stirrups in the service state: The load-deformation diagrams for models E1 and E2 in Figure 17 show that there is no noticeable improvement when varying the number of stirrups in the BCJ. However, other authors conclude that stirrups do play a fundamental role in the performance of the BCJ. Overall, it can be concluded that the effect of stirrups is not apparent in the ELS, being relevant only in Ultimate Limit State (ULS) loading stages [11].

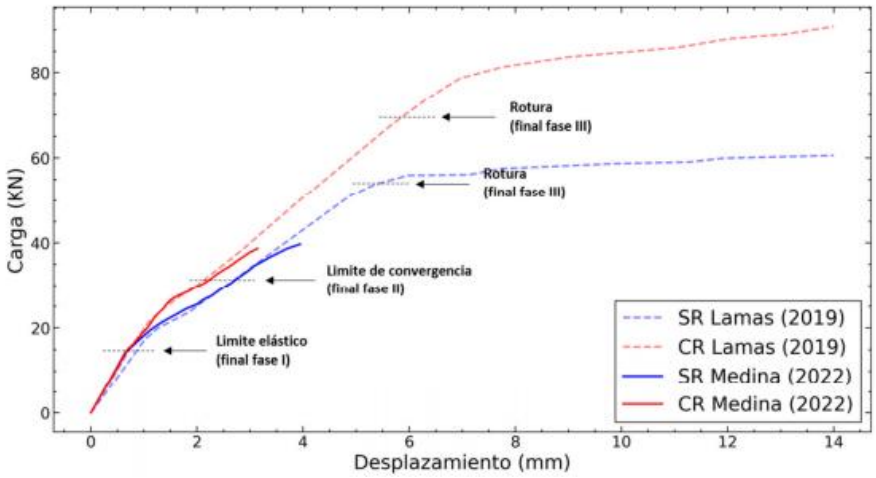


Figure 16. Load-displacement diagrams for the SR and CR models

(c) Study of the joint's behavior under the influence of different numbers of additional vertical bars in the service condition: The results shown in Figure 18 for models V1, V2, and V3 indicate that the vertical bars do not significantly improve the stiffness of the BCJ. This result is consistent with the comments made by Kassem [13] regarding this type of reinforcement that passes through the column along its axis. However, other authors report the opposite based on experimental studies they have conducted. According to Kassem [13], this contradiction also exists in the codes; for

example, the ACI does not consider the effect of vertical shear or any reinforcement for this zone, whereas the Eurocode recommends a minimum limit for the amount of reinforcement in the middle of the column.

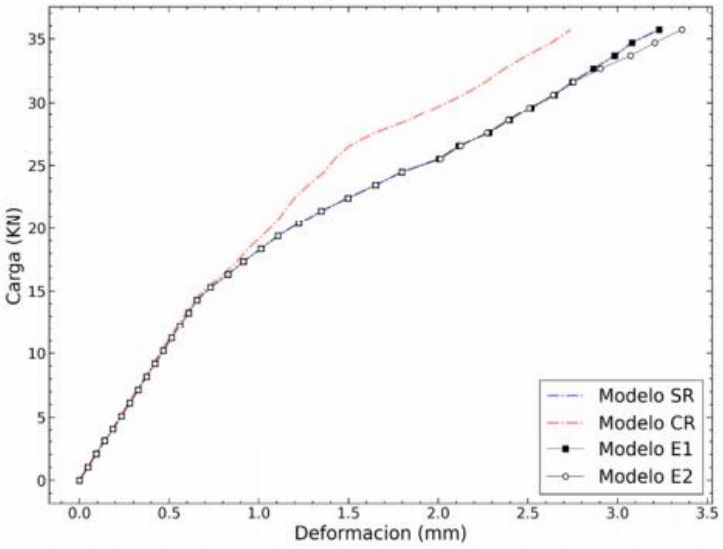


Figure 17. Load-displacement diagrams for models E1 and E2

(d) Study of the behavior of the beam region near the node under the influence of additional open stirrups: In the load-displacement diagrams in Figure 19, it can be observed that there is a noticeable improvement depending on the position and number of open stirrups: Model H3, which has three stirrups distributed throughout the entire height of the beam, shows better results than models H1 and H2. This indicates that the upper and lower stirrups perform better in combination than they do individually, as seen in models H1 and H4.

Models H2 and H4 exhibit similar behavior, suggesting that the use of the lower stirrup (in the beam's compression zone) does not significantly influence the joint's behavior. In contrast, stirrups located in the upper half of the beam's height show performance similar to that of Model H3, which has stirrups distributed throughout the entire height of the beam.

The H5 model performs similarly to the H3 model, which again demonstrates that stirrups located at the bottom of the beam do not improve the behavior of the BCJ. This makes the H5 model more efficient in terms of material utilization and construction, as using less steel facilitates the placement of concrete during pouring.

Model H6 increases the diameter of the bars but maintains the configuration of Model H5; this increase in steel quantity improves the mechanical response of the BCJ; thus, the greater the amount of steel in this region, the better the results obtained, provided that the position of the reinforcement is "ideal." The improvement resulting from the increased steel quantity in the BCJ would be limited by the minimum spacing required for the reinforcement by code, as applied in actual construction practice [20].

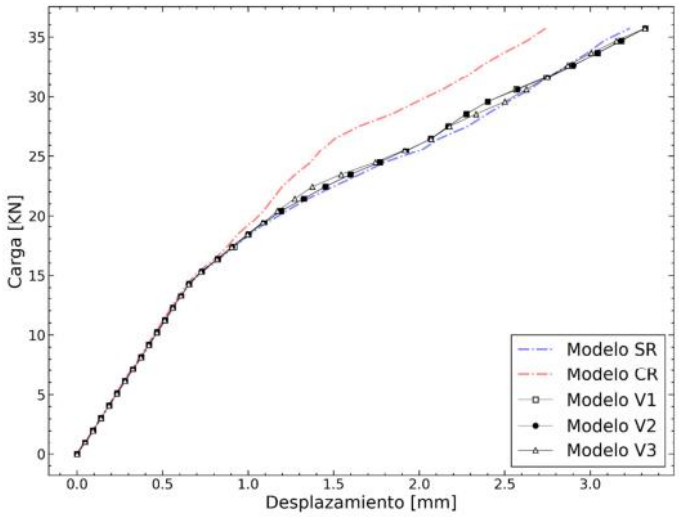


Figure 18. Load-displacement diagrams for models V1, V2, and V3

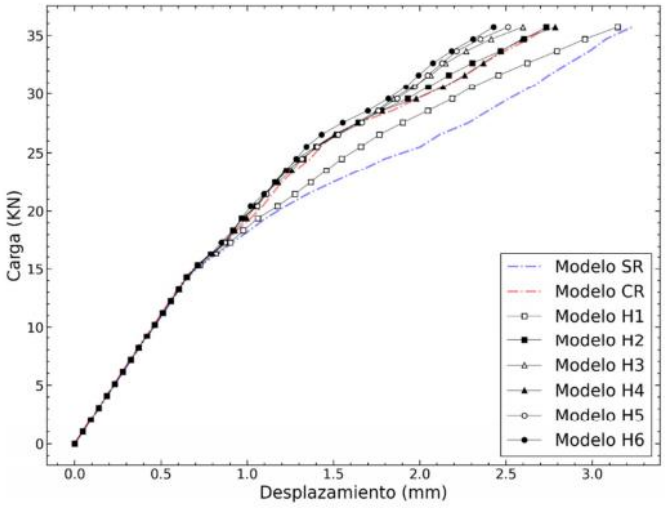


Figure 19. Load-displacement diagrams for models H1, H2, H3, H4, H5, and H6

Figure 20 shows a general comparison of the reinforcement configurations for models H5 and SR.

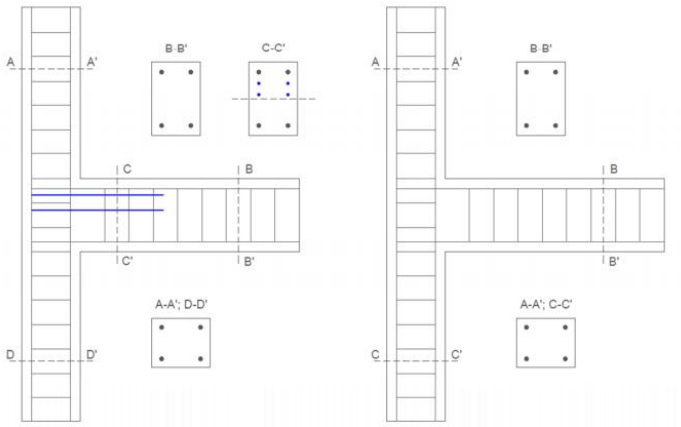


Figure 20. Comparison of reinforcement configurations between the H5 model (left) and that proposed by ACI 352 for Type 1 beam-to-column connections (right)

Figure 21 shows that the compressive stress in the concrete in the horizontal direction is lower in the H5 model than in the SR model. This occurs because the open stirrups resist part of the stress that the beam's main reinforcement resists. On the other hand, in the H5 model, the compression zones extend vertically toward the columns, whereas in the SR model they remain around the core, as shown in Figure 22. This results in higher stresses in the core and, consequently, earlier failure.

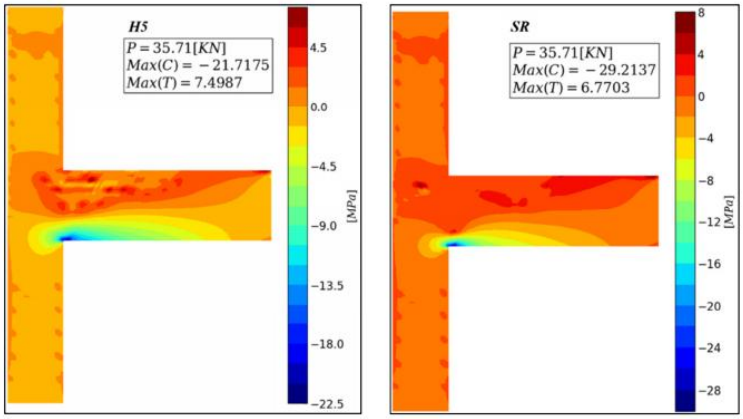


Figure 21. Normal stresses in concrete (σ_x [MPa]) H5 vs. SR models

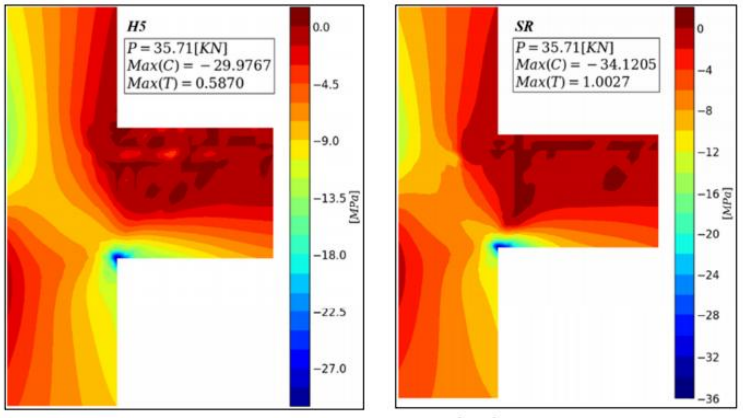


Figure 22. Principal stresses in the concrete (σ_2 [MPa]) H5 vs. SR models

The distribution of fractured elements at this loading stage shows that the reinforcement in the H5 model controls the propagation of cracks extending from the beam's tension zone to the compression zone, a phenomenon that impairs the stiffness of the beam-column connection [4], as can be seen in the comparison in Figure 23. Thus, it can be seen that the addition of open stirrups in the upper half of the beam's height improves the performance of the beam-column connection.

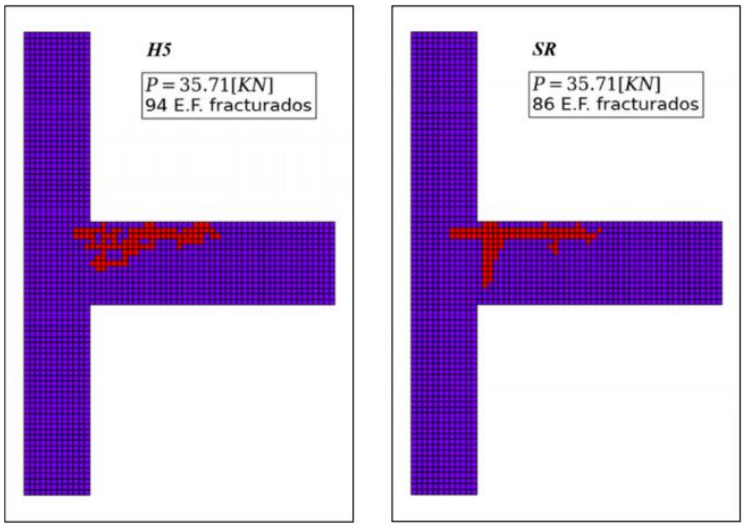


Figure 23. "Cracked" finite elements, H5 vs. SR models

Table 3 presents a summary of the comparative analysis between the H5 and SR models.

Table 3. Comparative summary between the H5 and SR models

Beam–Column Joint Typology	SR	H5	Dif.	%	Observation
Test Load [kN]	35.7	37.5	-	-	-
Maximum Deflection [mm]	3.43	2.71	0.72	21	Reduces
Fractured Elements	86	94	8	9.3	Increases
Maximum Normal Compressive Stress in Concrete in X Direction [MPa]	29.21	21.72	7.5	25.7	Reduces
Maximum Normal Tensile Stress in Concrete in X Direction [MPa]	6.77	7.5	0.73	10.8	Increases
Maximum Normal Compressive Stress in Concrete in Y Direction [MPa]	20.35	20.18	0.17	0.8	Reduces
Maximum Normal Tensile Stress in Concrete in Y Direction [MPa]	1.72	1.72	0	0	No change
Maximum Positive Shear Stress [MPa]	4.41	4.01	0.4	9.1	Reduces
Maximum Negative Shear Stress [MPa]	9.25	8.96	0.29	3.2	Reduces
Principal Stress S1 in Concrete [MPa]	10.7	10.7	0	0	No change
Principal Stress S2 in Concrete Core [MPa]	34.12	29.98	4.14	12.1	Reduces
Axial Compressive Stress of Main Beam Reinforcement [MPa]	79.25	73.11	6.14	7.8	Reduces
Axial Tensile Stress of Main Beam Reinforcement [MPa]	240.64	153.3	87.34	36.3	Reduces
Axial Compressive Stress of Main Column Reinforcement [MPa]	89.25	88.11	1.14	7.8	Reduces

8 Construction details of the H5 model

Finally, an exploded view and construction details of the reinforcement configuration proposed in this article, derived from the H5 model, are presented. Figure 24 shows that the only non-conventional reinforcement consists of open stirrups, which are strategically located in the beam's tension zone. There are two key parameters for the implementation of open stirrups: the diameter and spacing of the stirrups, and their effective length. Increasing the first parameter is inversely proportional to crack propagation, as shown in the results; however, this would be limited by the minimum spacing between reinforcement layers according to ACI 318, which is 25 mm. Regarding the second parameter, the standard specifies requirements for embedded length in concrete for tension bars; on the other hand, since this does not pertain to

the beam's longitudinal reinforcement, the applicability of this criterion must be studied.

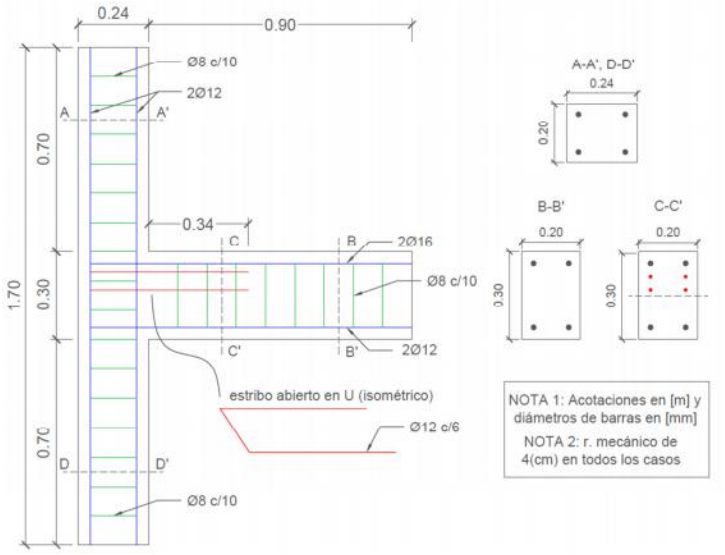


Figure 24. Construction detail of the H5 model. Open brackets shown in red

9 Conclusion

The results regarding the variation in the amount of closed stirrups in models E1 and E2 indicate that an increase in the amount of transverse reinforcement in the core does not improve the load-strain diagram at the serviceability limit state (Phases I and II).

Vertical reinforcement does not improve the performance of the beam-column connection during the linear elastic and cracking phases. This result is consistent with those obtained by other authors [21,22] regarding the limited influence that this type of reinforcement has on the strength of the beam-column connection [13].

The H5 model, featuring two open stirrups in the upper half of the beam's height, exhibits better mechanical performance than the SR model during Phases I and II (ELS) of reinforced concrete behavior [14]. This is because the open stirrups control the propagation of cracks that occur in the beam's tension zone toward the compression zone.

Placing the open stirrups in the upper half of the beam's depth is more efficient than distributing them throughout the entire depth of the beam, as it allows for easier construction.

Conflicts of interest

The author declares no conflicts of interest regarding the publication of this paper.

References

[1] C. R. Tipán Espinoza, «Modelización del comportamiento cíclico de uniones viga-columna de hormigón armado», Master's Thesis, Universitat Politècnica de Catalunya, 2019.

[2] A. Meseguer Garcia, F. Cabré Moran, y J. C. Portero Arroyo, Jimenez Montoya Hormigon armado, 15.a ed. Barcelona: Gustavo Gili, SL, 2011.

[3] V. G. Haach, «Análise teórico-experimental da influência da força normal em nós de pórtico externos de concreto armado», São Carlos Diss. Mestrado–Escola Eng. São Carlos Universidade São Paulo, 2005.

[4] G. M. S. Alva, «Estudo teórico-experimental do comportamento de nós de pórtico de concreto armado submetidos a ações cíclicas», São Carlos 218p Tese Doutorado–Escola Eng. São Carlos Universidade São Paulo, 2004.

[5] R. Kadarningsih, I. Satyarno, y A. Triwiyono, «Proposals of beam column joint reinforcement in reinforced concrete moment resisting frame: A literature review study», Procedia Eng., vol. 95, pp. 158-171, 2014.

[6] S. M. Alcocer, «Comportamiento y diseño de estructuras de concreto reforzado - Uniones de elementos», en Curso sobre seguridad sísmica de las construcciones para directores responsables de obra, México. Centro Nacional de Prevención de Desastres (CENAPRED), 1995, pp. 305-17.

[7] L. Salinas y E. Mercedes, «Análisis de elementos viga-columna en régimen no lineal con deformación por cortante», Diss Ind., 2015.

[8] R. Park y T. Paulay, Reinforced concrete structures. John Wiley & Sons, 1991.

[9] W. Roeser, «Zum tragverhalten von Rahmenknoten aus Stahlbeton», Lehrstuhl Inst. Für MassivBau RWTH Aachen Univ. Aachen Ger., 2002.

[10] R. T. Lamas, «Analisis Elastoplástico en la unión viga-columna de hormigon armado por el metodo de elementos finitos», Universidad Tecnica de Oruro, Oruro, 2019.

[11] I. R. de Ortiz, «Strut-and-tie modelling of reinforced concrete: short beams and beam-column joints», PhD Thesis, University of Westminster, 1993.

[12] A. C. I. Committee, «Recommendations for Design of Beam-Column Connections in Monolithic Reinforced Concrete Structures (ACI 352-02)», 2002.

[13] W. Kassem, «Strut-and-tie modelling for the analysis and design of RC beam-column joints», Mater. Struct., vol. 49, n.o 8, pp. 3459-3476, 2016.

[14] M. A. da S. Machado, «Aplicação do método dos elementos finitos para a análise elasto-viscoplástica de peças de concreto armado e protendido, submetidas a estados planos de tensão», 2002.

[15] B. M. Lazzari, «Análise por elementos finitos de peças de concreto armado e protendido sob estados planos de tensão», 2015.

[16] J. L. P. Tamayo, «Analise numérica de vigas mistas pelo método dos elementos finitos», 2011.

[17] S. M. Allam, M. S. Shoukry, G. E. Rashad, y A. S. Hassan, «Evaluation of tension stiffening effect on the crack width calculation of flexural RC members», Alex. Eng. J., vol. 52, n.o 2, pp. 163-173, 2013.

[18] I. Ergatoudis, B. M. Irons, y O. C. Zienkiewicz, «Curved, isoparametric,"quadrilateral" elements for finite element analysis», Int. J. Solids Struct., vol. 4, n.o 1, pp. 31-42, 1968.

[19] J. Romo Martin et al., «Metodo de Bielas y Tirantes - Monografia M6». ache, 2003.

[20] A. C. I. Committee, «Building code requirements for structural concrete (ACI 318-08) and commentary», 2008.

[21] S. Park y K. M. Mosalam, «Analytical and experimental study of RC exterior beam−column joints without transverse reinforcement», en Proceedings of the 7th international conference on urban earthquake engineering (7CUEE) & 5th international conference on earthquake engineering (5ICEE), 2010, vol. 803811.

[22] P. Sengupta y B. Li, «Modified Bouc−Wen model for hysteresis behavior of RC beam−column joints with limited transverse reinforcement», Eng. Struct., vol. 46, pp. 392-406, 2013.